Rice Hull Biocomposites, Part 2: Effect of the Resin Composition on the Properties of the Composite

Rafael L. Quirino, Richard C. Larock

Department of Chemistry, Iowa State University, Ames, Iowa 50011

Received 2 July 2010; accepted 22 November 2010
DOI 10.1002/app.33815
Published online 14 March 2011 in Wiley Online Library (wileyonlinelibrary.com).

ABSTRACT: A free radical thermoset resin consisting of a copolymer of conjugated linseed oil (CLO) or conjugated soybean oil (CSO), *n*-butyl methacrylate (BMA), divinylbenzene (DVB), and maleic anhydride (MA) has been reinforced with rice hulls. Composites containing 70 wt % of the filler were compression molded, the conjugated oil content in the resin was kept constant at 50 wt %, and the relative amounts of BMA, DVB, and MA were varied to afford composites with different resin compositions. Tensile tests, DMA, thermogravimetric analysis, and Soxhlet extraction of the different composites prepared have been used to establish the relationship between resin composition and the properties of the composites. Overall, the mechanical properties tend to improve when MA is introduced into the resin. Scanning electron microscopy of selected samples showed a better filler–resin interaction for MA-containing composites and samples prepared from CLO exhibit better properties than those prepared from CSO. © 2011 Wiley Periodicals, Inc. J Appl Polym Sci 121: 2050–2059, 2011

Key words: composites; copolymerization; mechanical properties; conjugated vegetable oil; rice hulls

INTRODUCTION

With the shortage in petroleum and growing concerns about the environment, the use of biorenewable materials for the production of bioplastics and biocomposites has recently gained increasing attention. Natural oils, which consist of triglycerides often containing polyunsaturated carbon chains, represent a promising component in the preparation of biobased materials due to their ready availability and low cost.

In particular, linseed and soybean oils have been used as major components in various resin formulations. Semi-conducting materials have been prepared from a poly(urethane amide) of linseed oil blended with poly(1-naphthylamine).[1] Linseed oil monoglyceride maleates have been co-polymerized with styrene (ST) to form a matrix for wood flour composites.[2] Clay composites have also been prepared using a matrix where conjugated linseed oil (CLO) was co-polymerized with divinylbenzene (DVB) and acrylic acid (AA),[3] and a similar resin, containing linseed oil, DVB, ST, and AA, has also been studied.[4] Linseed oil has also been used as the starting material in the preparation of an AA-esterified monomer for later co-polymerization with ST.[5] Also, polyester amides have been made from linseed oil.[6] Along the same lines, polyurethanes,[7] an epoxy resin for glass fiber composites,[8] and multicomponent thermoset resins from soybean oil have been reported among several other reports not cited here.[9]

The high degree of unsaturation in these oils (~6 C—C per triglyceride for linseed oil and 4.5 for soybean oil) makes them very attractive as comonomers in free radical resins. The fatty acid composition of linseed oil follows: 4% stearic acid, 19% oleic acid, 15% linoleic acid, 57% linolenic acid, and 5% of other fatty acids,[10] whereas soybean oil consists of 14% palmitic acid, 4% stearic acid, 24% oleic acid, 52% linoleic acid, and 6% linolenic acid.[11] Despite the high number of carbon–carbon double bonds in these oils, it is known that a significantly higher reactivity toward free radical polymerization processes is attained upon conjugation of the carbon–carbon double bonds.[12] Our group has investigated resins formed by the free radical copolymerization of CLO with acrylonitrile and DVB,[10] and the thermal polymerization of CLO in the presence of ST and DVB.[13] The cationic polymerization of a modified linseed oil and dicyclopentadiene (DCPD) has also been studied by the Larock group[14] as well as various resins containing conjugated soybean oil (CSO).[15–17]

More recently, we have studied the reinforcement of a CSO-based thermoset matrix containing DVB

Correspondence to: R. C. Larock (larock@iastate.edu).
Contract grant sponsor: Recycling and Reuse Technology Transfer Center of the University of Northern Iowa.

and *n*-butyl methacrylate (BMA) with corn stover[18] and soybean hulls.[19] In the latter system, DCPD was employed in the resin to partially substitute either DVB or BMA in an attempt to improve the mechanical properties and lower the cost of the resulting composite. A similar resin, containing unmodified tung oil, has been reinforced with spent germ by us.[20,21]

Rice hulls are a major agricultural by-product from the rice industry and very few uses have been proposed for it. It normally ends up being disposed of in landfills or just burned to produce an ash rich in silica.[22] The use of rice hulls as a reinforcement for polypropylene composites has been reported recently, and the promising results suggest that it may work as a good filler in the preparation of bio-based composites.[23] The preparation of rice hull composites from CLO has been optimized in Part 1 of this project.[24] The effect of cure sequence, pressure, filler load, particle size, and drying of the filler on the composite properties has been studied, and the best conditions for preparation of these rice hull-reinforced materials have been established.[24]

In this project, we report the preparation of rice hull composites with resins of various compositions. All of the resins studied here contain 50 wt % of the conjugated vegetable oil and different concentrations of maleic anhydride (MA), BMA, and DVB. MA, in this system, acts as a compatibilizer between the hydrophobic matrix and the hydrophilic filler. The effect of the concentration of the different comonomers used on the final composite properties has been assessed by means of tensile tests, dynamic mechanical analysis (DMA), thermogravimetric analysis (TGA), Soxhlet extraction, scanning electron microscopy (SEM), and proton nuclear magnetic resonance spectroscopy (^{1}H-NMR).

EXPERIMENTAL

Materials

BMA was purchased from Alfa Aesar (Ward Hill, MA). DVB, MA, and *t*-butyl peroxide (TBPO) were purchased from Sigma-Aldrich (St. Louis, MO). All were used as received. Superb linseed oil was provided by ADM (Red Wing, MN) and soybean oil (Great Value brand, Bentonville, AR) was purchased in a local grocery store. Both oils have been conjugated using a rhodium catalyst, following a method developed and frequently used by our group.[12] The rice hulls were provided by the Missouri Crop Improvement Association (Columbia, MO). They were ground to <1 mm diameter particle size and dried overnight at 70°C in a vacuum oven before use.

General procedure for preparation of the composites

The crude resin was obtained by mixing the conjugated vegetable oil, BMA and DVB in a beaker. MA was melted in a hot water bath and quickly added to the crude resin mixture under agitation, along with the free radical initiator TBPO. The rice hulls were impregnated with the crude resin and compression molded for 5 h at 180°C and 600 psi. The composites were then removed from the mold and post-cured in a convection oven for 2 h at 200°C at ambient pressure. An optimal filler load of 70 wt % had been pre-established in Part 1 of this project and has been kept constant throughout Part 2.[24] In all composites produced, the resin has a conjugated vegetable oil content of 50 wt % and the optimal amount of TBPO has been determined to be, in preliminary tests, an extra 5 wt % of the total resin weight. The amounts of DVB, BMA, and MA have been varied, as indicated in the text, to produce composites of various compositions.

Characterization of the composites

Tensile tests were conducted at room temperature according to ASTM D-638 using an Instron universal testing machine (model 5569) equipped with a video extensometer and operating at a crosshead speed of 2.0 mm/min. Dogbone-shaped test specimens were machined from the original samples to give the following gauge dimensions: 57.0 mm × 12.7 mm × 4.5 mm (length × width × thickness, respectively). For each composite, seven dog-bones were cut and tested. The results presented in the text are the average of these measurements along with the calculated standard deviation.

DMA experiments were conducted on a Q800 DMA (TA Instruments, New Castle, DE) using a three point bending mode with a 15.0 mm clamp. Rectangular specimens of 22.0 mm × 8.5 mm × 1.5 mm (length × width × thickness, respectively) were cut from the original samples. Each specimen was cooled to −60°C and then heated at 3°C/min to 250°C. The experiment was conducted using a frequency of 1 Hz and an amplitude of 14 μm under air. Two runs for each sample were carried out, and the results presented in the text reflect the average of the two measurements.

A Q50 TGA instrument (TA Instruments, New Castle, DE) was used to measure the weight loss of the samples under an air atmosphere. The samples (~10 mg) were heated from room temperature to 650°C at a rate of 20°C/min.

Soxhlet extraction was conducted to determine the amount of soluble materials in the composites. A 2.0 g sample of each composite was extracted for 24 h

TABLE I
Tensile Tests and DMA Results for Biocomposites Made from Conjugated Linseed Oil (CLO)

Entry	BMA (wt %)	DVB (wt %)	MA (wt %)	Young's modulus (GPa)	Tensile strength (MPa)	Storage modulus at 130°C (MPa)	T_g (°C)
1	35	15	–	2.3 ± 0.5	5.9 ± 0.6	220	52
2	35	10	5	1.9 ± 0.4	7.9 ± 1.6	609	64
3	35	5	10	1.9 ± 0.3	7.1 ± 1.0	391	45
4	35	–	15	1.7 ± 0.4	5.8 ± 0.9	345	33
5	30	15	5	2.1 ± 0.7	7.0 ± 1.3	141	0, 69[a]
6	25	15	10	2.1 ± 0.3	8.4 ± 1.2	350	63
7	20	15	15	2.3 ± 0.4	9.1 ± 1.7	255	75
8	30	10	10	1.7 ± 0.5	7.8 ± 1.3	332	71
9	30	5	15	2.1 ± 0.6	8.0 ± 1.3	258	68
10	25	10	15	1.8 ± 0.3	7.7 ± 1.0	476	78

[a] Two T_g's were observed.

with dichloromethane (CH_2Cl_2). After extraction, the solubles were recovered by evaporating the CH_2Cl_2 under vacuum. Both soluble and insoluble materials were dried overnight at 70°C. The dried soluble fraction was then dissolved in deuterated chloroform ($CDCl_3$), and the ^{1}H-NMR spectrum was obtained using a Varian Unity spectrometer (Varian Associates, Palo Alto, CA) operating at 300 MHz. The ^{1}H-NMR spectra helped to determine the identity of the solubles in each sample.

For the SEM analysis, each sample was frozen with liquid nitrogen prior to fracture (cryofracture). A second section of the sample was mechanically cut and shaved with a razor blade to provide a smooth cross section. Both cryofractured and cut samples were examined using an Hitachi S-2460N variable-pressure SEM. The microscope was operated at 20 kV accelerating voltage, with 60 Pa of helium atmosphere, and a 25 mm working distance. Backscattered electron images were collected using a Tetra BSE detector (Oxford Instruments) at 35× and 100× magnifications.

RESULTS AND DISCUSSION

Mechanical properties of CLO-containing composites

The tensile test and DMA results of all samples made with CLO are summarized in Table I. Young's moduli, tensile strengths, storage moduli at 130°C, and T_g's are reported for the CLO-containing composites with different resin compositions.

Comparing entries 1–4 in Table I, the effect of gradual substitution of DVB by MA on the mechanical properties can be assessed. There is an overall decrease in Young's modulus (E) from 2.3 GPa to 1.7 GPa when 15 wt % DVB is replaced by MA (entries 1 and 4, respectively, Table I). Although the loss in E is not dramatic, it reveals that DVB is probably the component mainly responsible for the stiffness of the resin. A similar trend was observed when DVB was replaced by DCPD in soybean hull composites.[19]

The tensile strength of the composites exhibits a different trend upon gradual substitution of DVB by MA (entries 1–4, Table I). There is an increase in the tensile strength for the samples containing 5 wt % and 10 wt % MA (7.9 MPa and 7.1 MPa, respectively, entries 2 and 3, Table I) in comparison with the sample where MA is completely absent (5.9 MPa, entry 1, Table I). This reveals that MA behaves as a compatibilizer between the resin and the filler in this system. Indeed, the C—C double bond in MA can be co-polymerized with the resin, whereas the anhydride group can be opened by the hydroxyl groups present in the cellulose and hemicellulose in the rice hulls at the high temperatures employed during the cure. With a better filler–resin interaction whenever MA is present, there is better stress transfer from the matrix to the filler, resulting in a higher tensile strength for the composite. For entry 4 (Table I), the decrease in tensile strength (5.8 MPa) is related to the absence of DVB in the resin. In this case, the loss in mechanical properties due to the absence of DVB is not compensated for by the better filler–resin interaction imparted by the presence of MA.

A similar trend is observed for the storage modulus at 130°C (E') and the T_g of the samples when substituting DVB by MA (entries 1–4, Table I). In both cases, there is an increase in the value when 5 wt % MA is introduced into the resin (entry 2, Table I). E' increases from 220 MPa to 609 MPa, whereas T_g increases from 52°C to 64°C (entries 1 and 2, Table I). As mentioned earlier, this increase is related to a better filler–resin interaction imparted by the presence of the MA. When the amount of

DVB in the resin is below 10 wt % (entries 3 and 4, Table I), a decrease in E' from 609 MPa (entry 2) to 345 MPa (entry 4) and T_g from 64°C (entry 2) to 33°C (entry 4) is observed, due to the loss in rigidity of the system.

When BMA is gradually substituted by MA, (entries 1 and 5–7, Table I) the Young's modulus is not significantly affected, which reveals that, structurally, both molecules have similar characteristics. On the other hand, the tensile strength increases remarkably from 5.9 MPa (entry 1, Table I) to 9.1 MPa (entry 7, Table I) when BMA is substituted by MA, showing, once again, the better filler–resin effect imparted by MA. No specific trend could be distinguished for the storage modulus at 130°C when BMA was substituted by MA. There is an overall increase in T_g from 52°C (entry 1, Table I) to 75°C (entry 7, Table I) by substituting BMA with MA. The appearance of two T_g's (entry 5, Table I) is not completely understood. In our previous work with soybean hulls,[19] the appearance of two T_g's was related to the presence of comonomers with distinctly different reactivities (e.g., CSO, BMA, and DVB).

When 5 wt % of DVB and 5 wt % of BMA are replaced with 10 wt % of MA, there is a decrease in Young's modulus from 2.3 GPa (entry 1, Table I) to 1.7 GPa (entry 8, Table I) due to the decrease in DVB content, as explained earlier. The tensile strength, storage modulus at 130°C and T_g increase from 5.9 MPa, 220 MPa, and 52°C to 7.8 MPa, 332 MPa, and 71°C, respectively. These variations show, once again, the gain in mechanical properties due to the addition of MA to the resin and the better filler–resin interaction. When an additional 5 wt % of DVB is replaced by MA (entry 9, Table I), the tensile properties are not significantly affected, since the difference in the Young's modulus and the tensile strength between entries 8 and 9 (Table I) falls within the standard deviation of the measurements. On the other hand, the storage modulus at 130°C and the T_g decrease from 332 MPa and 71°C (entry 8, Table I) to 258 MPa and 68°C (entry 9, Table I), respectively.

Finally, the tensile properties of the sample with 25 wt % of BMA, 10 wt % of DVB, and 15 wt % of MA (entry 10, Table I) are comparable with those of the sample in entry 8, Table I. The difference in E and tensile strength fall within the standard deviation of the experiment and can be neglected. The only significant differences occur in the storage modulus at 130°C, with an increase from 332 MPa (entry 8, Table I) to 476 MPa and in T_g, with an increase from 71°C (entry 8, Table I) to 78°C.

The curves showing loss modulus (E'') versus temperature for selected formulations are given in Figure 1. For all of the curves shown, there is an overall

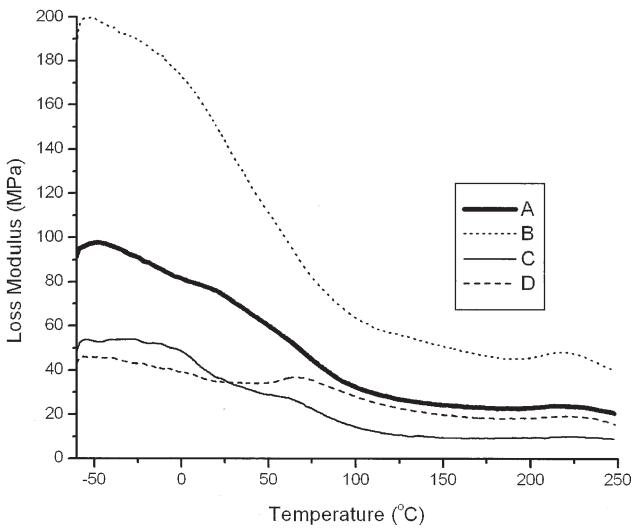

Figure 1 Loss modulus versus temperature for rice hull-reinforced composites with selected formulations: (A) 50 wt % CLO, 35 wt % BMA, and 15 wt % DVB; (B) 50 wt % CLO, 35 wt % BMA, 10 wt % DVB, and 5 wt % MA; (C) 50 wt % CLO, 30 wt % BMA, 15 wt % DVB, and 5 wt % MA; (D) 50 wt % CLO, 20 wt % BMA, 15 wt % DVB, and 15 wt % MA.

decrease in loss modulus with an increase in temperature. This behavior is most likely the result of further reaction of the remaining carbon–carbon double bonds in the resin, which increases the crosslink density and gradually inhibits the dissipation of the energy through movement of the polymer chains. It is interesting to observe that the loss modulus plateaus at ~120°C, when all carbon–carbon double bonds in the resin have, most likely, reacted. In the case of the sample containing 10 wt % DVB [Fig. 1(B)], the lower amount of the crosslink agent results in a higher loss modulus, when compared to the other curves in Figure 1, for the entire temperature range studied. Indeed, if a lower crosslink density is attained, the polymer chains in the matrix are more free to dissipate the stress energy into movement, resulting in a higher loss modulus. For samples with the same DVB content [Fig. 1(A,C,D)], one can correlate the loss modulus behavior with the presence of MA in the resin. When MA is present [Fig. 1(C,D)], the resulting better filler–resin interaction provides more efficient stress transfer from the matrix to the reinforcement, preventing significant dissipation of energy into polymer chain motion, and as a consequence, a decrease in the loss modulus is observed [compare with Fig. 1(A)]. When comparing Figure 1(C,D), a logical relationship between the amount of MA in the resin and the loss modulus can be established for temperatures lower than 25°C. With a higher MA content, Figure 1(D) exhibits a lower loss modulus for the reasons already discussed. However, an interesting inversion of the loss

TABLE II
TGA and Soxhlet Extraction Results for Biocomposites Made from Conjugated Linseed Oil (CLO)

Entry	BMA (wt %)	DVB (wt %)	MA (wt %)	T_{10} (°C)	T_{50} (°C)	T_f (°C)	Residue (wt %)	Solubles (wt %)[a]	Insolubles (wt %)[a]
1	35	15	–	304	426	606	15	5	95
2	35	10	5	300	408	635	11	4	96
3	35	5	10	304	419	611	11	5	95
4	35	–	15	299	420	595	12	6	94
5	30	15	5	304	425	614	11	4	96
6	25	15	10	306	433	599	11	5	95
7	20	15	15	305	433	638	11	4	96
8	30	10	10	302	418	601	11	5	95
9	30	5	15	304	413	622	11	5	95
10	25	10	15	301	416	607	10	5	95

[a] Determined by Soxhlet extraction using CH_2Cl_2 for 24 h.

modulus behavior is observed after 25°C. This phenomenon may be related to the overall reactivity of the resin components. Indeed, the loss modulus decreases from 43 MPa to 18 MPa over the temperature range studied and shown in Figure 1(D), whereas, for Figure 1(C), the decrease observed is from 49 MPa to 9 MPa, suggesting that more carbon–carbon double bonds remain unreacted for resins containing less MA.

Thermal properties and Soxhlet extraction results of CLO-containing composites

The TGA and Soxhlet extraction results are summarized in Table II. T_{10} corresponds to the temperature required to attain loss of 10 wt % of the initial sample; T_{50} corresponds to the temperature required to attain loss of 50 wt % of the initial sample; and T_f corresponds to the temperature after which no further weight loss was detected.

From the results in Table II, it can be seen that the changes in T_{10} are very subtle, when comparing composites with different resin compositions. Indeed, the T_{10} values vary only from 299°C (entry 4, Table II) to 306°C (entry 6, Table II) with no obvious trend, leading to the conclusion that this initial 10 wt % loss is not related to any component of the resin. It could be related, in fact, to initial degradation of the hemicellulose from the rice hulls.[25]

For the T_{50} values, however, some general trends can be identified. For example, samples with 15 wt % of DVB exhibit a T_{50} value that varies from 425°C (entry 5, Table II) to 433°C (entries 6 and 7, Table II). When the DVB content is below 15 wt %, the T_{50} value ranges from 413°C (entry 9, Table II) to 420°C (entry 4, Table II), the exception being entry 2 in Table II (408°C). This suggests that DVB, with its higher reactivity in free radical polymerization processes, is readily polymerized. Therefore, samples with a higher DVB content possess a network with a higher crosslink density and, as a consequence, higher temperatures are required to attain a loss of 50 wt %.

Only a few trends could be distinguished when analyzing the T_f values obtained for the composites prepared in this work. By comparison of entries 1 and 2 in Table II, it can be seen that substitution of 5 wt % of DVB by MA imparts an increase in T_f from 606°C to 635°C. This increase is probably related to the better interaction between filler and matrix after addition of MA, which gives the material a lower rate of weight loss in the later stages of thermal degradation. The same analysis can be made when comparing entries 1 and 5 in Table II. In this case, substitution of 5 wt % of BMA by MA also imparts an increase in the T_f value, from 606°C to 614°C. These observations correlate well with the results for the tensile strength (entries 1, 2, and 5, Table I). Comparing entries 2–4 in Table II, the T_f value decreases with the percentage of DVB in the resin, from 635°C (entry 2, Table II) to 595°C (entry 4, Table II). The results summarized in entries 1 and 8 (Table II) show a very similar thermal degradation profile for the corresponding samples. As mentioned earlier, the loss in thermal stability by the lower amount of DVB in entry 8 is compensated for by the addition of MA, which gives a better matrix-filler interaction. For entries 6, 7, 9, and 10 (Table II), no specific trend is observed with a variation in the resin composition.

The TGA and DTA curves of some selected formulations, along with the data for pure rice hulls, are given in Figure 2. The TGA curves shown in Figure 2(B,C) are representative of all MA-containing composites. For those samples, little variation in the residue left after thermal degradation is observed independent of the changes in resin composition. As discussed earlier, the rice hulls are the main source of residue in these composites. Figure 2(D) shows that ~18 wt % of the residue is left after thermal degradation of the rice hulls alone. This relatively high residue content has been associated with the

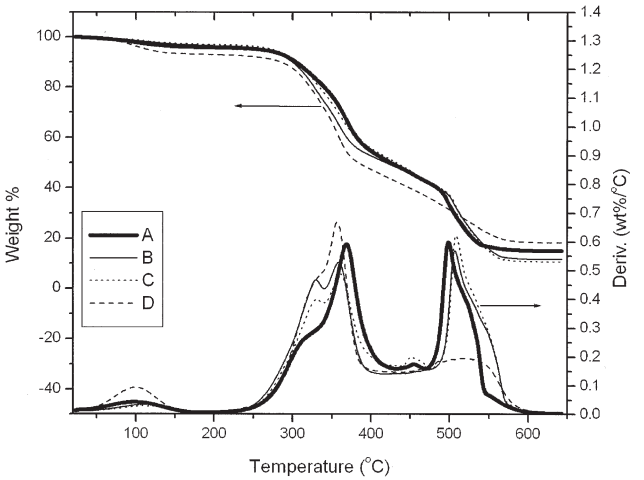

Figure 2 TGA and DTA curves for rice hull-reinforced composites with selected formulations: (A) 50 wt % CLO, 35 wt % BMA, and 15 wt % DVB; (B) 50 wt % CLO, 35 wt % BMA, and 15 wt % MA; (C) 50 wt % CLO, 20 wt % BMA, 15 wt % DVB, and 15 wt % MA; and pure rice hulls (D).

presence of significant amounts of silica on the surface of the rice hulls.[24] When comparing all of the resin formulations studied here, it can be observed that when no MA is present in the resin [entry 1, Fig. 2(A) and Table II], a higher percentage of residue is left after thermal degradation. The close interaction of the anhydride groups in MA with the hydroxyl groups from cellulose and hemicellulose on the surface of the rice hulls may facilitate the degradation of the filler particles during the TGA experiment. For all of the other formulations, the variation in residue left after TGA is insignificant (Table II).

The DTA curves in Figure 2 show that the thermal degradation of the materials occurs in five distinct steps. The first step, around 100°C, consists of loss of water from the rice hulls. The second step, occurring at 330°C has two components, one associated with degradation of the hemicellulose from the rice hulls[25] [clearly observed in Fig. 2(A,D)] and another associated with the degradation of MA. This latter component can be easily identified in Figure 2(B,C). The third step occurs between 360°C and 370°C and is associated with degradation of the cellulose from the rice hulls.[25] It is therefore present in all curves shown in Figure 2. The fourth step, at 455°C, is only seen in Figure 2(A,C), and can be associated with degradation of the DVB component of the resin. The last step occurs between 490°C and 550°C, and can be associated with the dissociation of carbon–carbon bonds from the lignin in the rice hulls[25] and the vegetable oil in the resin.

Finally, all of the composites presented in Table II afforded 4–6 wt % of soluble materials after Soxhlet extraction with CH_2Cl_2 for 24 h. Considering that the rice hulls alone afford 10 wt % of soluble material (data not shown in Table II),[24] this indicates that the majority of the resin components were incorporated into the resin during the cure and that a high crosslink density has been attained with essentially no differences between the various composite samples.

SEM study of rice hull-reinforced composites

The SEM images of cut and cryofractured composites with different resin compositions is shown in Figure 3. Figure 3(A,B) shows the cut cross section of composites where the resin composition is 50 wt % CLO, 35 wt % BMA, and 15 wt % DVB; and 50 wt % CLO, 20 wt % BMA, 15 wt % DVB, and 15 wt % MA, respectively. A comparison of Figure 3(A,B) reveals visual evidence of the better resin-filler interaction obtained when MA is added to the resin. Indeed, a greater number of voids can easily be seen in Figure 3(A). Furthermore, Figure 3(B) indicates an overall better dispersion of the rice hull particles in the matrix. These observations are in agreement with the results in Tables I and II.

Figure 3(C,D) show the cryofractured cross section of the same composites shown in Figure 3(A,B) at a higher magnification (100×). Here, again, it is possible to confirm the better filler–resin interaction obtained when MA is used as a comonomer in the resin. In Figure 3(C), a gap can be seen between the resin and the filler particles, whereas in Figure 3(D), it is almost impossible to discern any discontinuity in the interface between the resin and the filler.

Comparison of the properties of CSO- and CLO-containing composites

Table III summarizes the tensile test and DMA results for composites made from CSO and CLO. There is an increase in the tensile strength whenever 15 wt % of BMA is substituted by MA, independent of the oil used. For the CSO-containing samples, the tensile strength increases from 4.2 MPa to 7.0 MPa when MA is added to the resin (entries 1 and 2, Table III). For the CLO-containing samples, the tensile strength increases from 5.9 MPa to 9.1 MPa (entries 3 and 4, Table III). As mentioned earlier, MA acts as a compatibilizer between the matrix and the filler, helping in stress transfer and therefore improving the tensile strength. An increase in Young's modulus from 1.2 to 2.2 GPa (entries 1 and 2, Table III) is also observed when BMA is partially replaced by MA in the CSO-containing composites. For CLO-containing composites, there is no change in E upon substitution of BMA by MA (2.3 GPa, entries 3 and 4 in Table III). As expected, the use of CLO gives

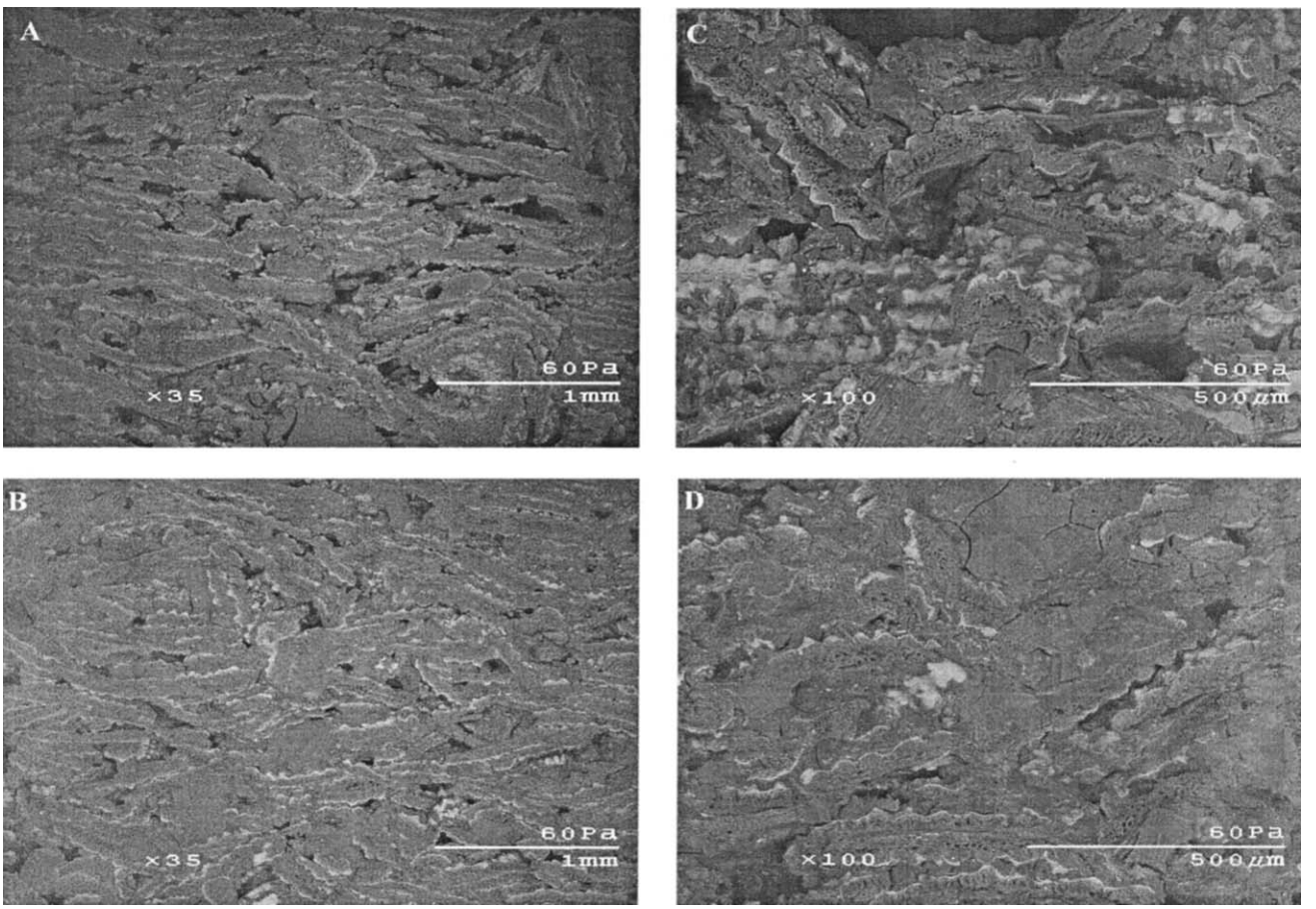

Figure 3 SEM images of: (A) cross section of a cut rice hull-reinforced composite (×35 magnification) with resin composition 50 wt % CLO, 35 wt % BMA, and 15 wt % DVB; (B) cross section of a cut rice hull-reinforced composite (×35 magnification) with resin composition 50 wt % CLO, 20 wt % BMA, 15 wt % DVB, and 15 wt % MA; (C) cross section of a cryofractured rice hull-reinforced composite (×100 magnification) with resin composition 50 wt % CLO, 35 wt % BMA, and 15 wt % DVB; (D) cross section of a cryofractured rice hull-reinforced composite (×100 magnification) with resin composition 50 wt % CLO, 20 wt % BMA, 15 wt % DVB, and 15 wt % MA.

composites with better tensile properties than those made from CSO. In the absence of MA, the Young's modulus and the tensile strength increase, respectively, from 1.2 GPa and 4.2 MPa to 2.3 GPa and 5.9 MPa (entries 1 and 3 in Table III) by changing the oil in the resin composition from CSO to CLO. The same is observed for the composites containing MA. *E* and the tensile strength increase from 2.2 GPa and 7.0 MPa to 2.3 GPa and 9.1 MPa, respectively (entries 2 and 4 in Table III). This effect is related to the higher number of carbon–carbon double bonds present in the linseed oil compared with soybean oil. The higher degree of unsaturation of linseed oil results in a resin with a higher crosslink density.

An increase in storage modulus is also observed when 15 wt % of BMA is replaced by MA. In composites containing CSO, the increase is more substantial (from 215 MPa to 613 MPa, entries 1 and 2

TABLE III
Tensile Tests and DMA Results for Biocomposites Made from Conjugated Linseed Oil (CLO) and Conjugated Soybean Oil (CSO)

Entry	Oil (50 wt %)	BMA (wt %)	DVB (wt %)	MA (wt %)	Young's modulus (GPa)	Tensile strength (MPa)	Storage modulus at 130°C (MPa)	T_g (°C)
1	CSO	35	15	–	1.2 ± 0.3	4.2 ± 0.7	215	24, 78[a]
2	CSO	20	15	15	2.2 ± 0.9	7.0 ± 1.2	613	0, 92[a]
3	CLO	35	15	–	2.3 ± 0.5	5.9 ± 0.6	220	52
4	CLO	20	15	15	2.3 ± 0.4	9.1 ± 1.7	255	75

[a] Two T_g's were observed.

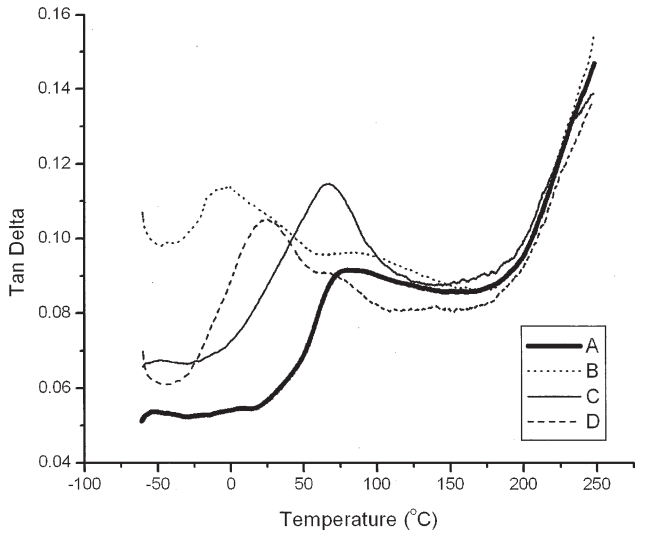

Figure 4 Tan δ curves of: (A) rice hull-reinforced composite with resin composition 50 wt % CLO, 20 wt % BMA, 15 wt % DVB, and 15 wt % MA; (B) rice hull-reinforced composite with resin composition 50 wt % CSO, 20 wt % BMA, 15 wt % DVB, and 15 wt % MA; (C) rice hull-reinforced composite with resin composition 50 wt % CLO, 35 wt % BMA, and 15 wt % DVB; (D) rice hull-reinforced composite with resin composition 50 wt % CSO, 35 wt % BMA, and 15 wt % DVB.

in Table III) than in those containing CLO (from 220 to 255 MPa, entries 3 and 4 in Table III). The effect of the oil on the storage modulus isn't clear as an increase from 215 to 220 MPa is observed when CSO is replaced by CLO in MA-free composites (entries 1 and 3 in Table III), whereas a substantial decrease from 613 MPa to 255 MPa is observed for the MA-containing composites (entries 2 and 4 in Table III).

The glass transition temperatures measured by DMA and reported in Table III reveal an interesting phenomenon observed in previous studies.[19] The presence of two very distinct T_g's for CSO-containing samples indicates that there is, most likely, a phase separation of the resin during polymerization of the different comonomers. Because of its lower reactivity in comparison to CLO, CSO polymerizes at a slower rate during the cure of the resin. This slower polymerization rate results in an initially formed phase which is richer in the more reactive comonomers, such as DVB. When most of the DVB is polymerized, a CSO-rich phase starts to form, thereby explaining the two T_g's observed.

The tan δ curves of samples containing CSO and CLO are shown in Figure 4. Figure 4(A) is representative of all resin compositions containing CLO and MA (Table I). The CSO-containing composites [Fig. 4(B,C)] exhibit two tan δ peaks, which is indicative of a possible phase separation that results in two distinct T_g values, as discussed earlier. The first peak is very obvious and occurs at temperatures lower than 50°C, whereas the second transition is less obvious and occurs at higher temperatures. When comparing composites made with the same vegetable oil [Fig. 4(A,C), for example], sharper tan delta peaks are obtained when MA is not a part of the formulation. This result implies that although a better filler–resin interaction is obtained when MA is added to the resin, a more heterogeneous matrix is formed. The difference in reactivity between the vegetable oil and the other comonomers may result in an initially formed oil-poor phase containing anhydride units that can strongly interact with the filler particles. The interaction between MA and the rice hulls compromises the overall dispersion of growing polymer chains among the filler particles, resulting in a more heterogeneous polymer phase.

Table IV presents the TGA and extraction data for composites containing CSO and CLO. Little variation was found for the T_{10} values of the composites listed in Table IV, with a maximum T_{10} value of 306°C for the CSO-containing composite without MA and a minimum of 301°C for the CSO-containing composite with MA (entries 1 and 2 in Table IV). As discussed previously, this initial 10 wt % loss is related to initial degradation of the filler, and therefore, switching from CLO to CSO should have no effect on the T_{10} value.

The T_{50} values, on the other hand, show a close relationship to the resin composition. There is an increase in the T_{50} value whenever MA is added to the resin. For CSO-containing composites, the T_{50} value increases from 405°C to 419°C (entries 1 and 2

TABLE IV
TGA and Soxhlet Extraction Results for Biocomposites Made from Conjugated Linseed Oil (CLO) and Conjugated Soybean Oil (CSO)

Entry	Oil (50 wt %)	BMA (wt %)	DVB (wt %)	MA (wt %)	T_{10} (°C)	T_{50} (°C)	T_f (°C)	Solubles (wt %)[a]	Insolubles (wt %)[a]
1	CSO	35	15	–	306	405	592	4	96
2	CSO	20	15	15	301	419	600	4	96
3	CLO	35	15	–	304	426	606	5	95
4	CLO	20	15	15	305	433	638	4	96

[a] Determined by Soxhlet extraction using CH_2Cl_2 for 24 h.

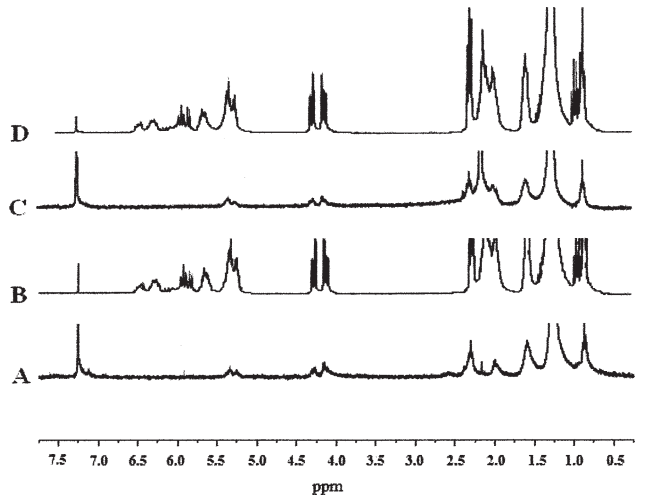

Figure 5 ^{1}H-NMR spectra of: (A) extract of a rice hull biocomposite with resin composition 50 wt % CLO, 35 wt % BMA, and 15 wt % DVB; (B) conjugated linseed oil; (C) extract of a rice hull biocomposite with resin composition 50 wt % CSO, 20 wt % BMA, 15 wt % DVB, and 15 wt % MA; (D) conjugated soybean oil.

in Table IV), while the increase in CLO-containing composites occurs from 426°C to 433°C (entries 3 and 4 in Table IV). This behavior was previously attributed to the better filler–resin interaction imparted by the presence of MA. When the T_{50} values of CSO- and CLO-containing composites are compared, it becomes evident that CLO gives higher numbers. Indeed, there is an increase in the T_{50} value from 405°C to 426°C when CSO is substituted by CLO in MA-free composites (entries 1 and 3 in Table IV). Also, an increase from 419°C to 433°C in the T_{50} value is seen when CLO substitutes CSO in MA-containing composites (entries 2 and 4 in Table IV). As mentioned earlier, CLO is expected to give a resin with a higher crosslink density than CSO, which would account for the higher temperatures required to attain 50 wt % degradation.

The T_f values for the samples listed in Table IV exhibit a very similar trend to the T_{50} values. An increase in the T_f value was detected whenever MA is added to the resin (from 592°C to 600°C for the CSO-containing composites and from 606°C to 638°C for the CLO-containing composites, entries 1 and 2, and 3 and 4 in Table IV). Also, an increase in T_f is observed when CSO is replaced by CLO (from 592°C to 606°C for the MA-free composites and from 600°C to 638°C for the MA-containing samples; entries 1 and 3, and 2 and 4 in Table IV).

The percentage of solubles determined by Soxhlet extraction of the composites does not reveal much, since only a minimal variation was detected. All samples analyzed afforded 4–5 wt % of soluble material (Table IV), thus showing that the amount of material retained in the composite after extraction is not strongly dependent on the resin composition variations introduced here. The Soxhlet extraction results reflect how much of the monomers have been incorporated into the matrix. In fact, both CSO and CLO can crosslink, to different degrees, through their multiple carbon–carbon double bonds. So no significant variations in the extraction results were expected among the samples shown in Table IV. From the ^{1}H-NMR spectra of the extracts of selected samples, it can be clearly seen that the soluble content recovered from the composites [Fig. 5(A,C)] resembles the unreacted CLO and CSO [Fig. 5(B,D), respectively]. The methylene hydrogen peaks between 4.0 ppm and 4.5 ppm in Figure 5(A,B) confirm the presence of a triglyceride unit in the extract. The absence of other distinctive peaks in the spectra indicates that, with the exception of the conjugated oil, all the other co-monomers are fully incorporated into the cured resin.

CONCLUSIONS

Rice hull-reinforced composites have been prepared by the free radical polymerization of resins with different compositions. The resins used had a constant conjugated vegetable oil (CLO or CSO) content of 50 wt % and a variable amount of BMA, DVB, and MA. The pressure, cure sequence, filler load, and particle size were kept constant. Tensile tests, DMA, and TGA experiments showed an overall improvement in the composites' properties whenever MA was added as a co-monomer in the resin. MA acts as a compatibilizer between the filler particles and the matrix. These results have been corroborated by SEM images showing a better filler–resin interaction in composites where the matrix contains MA. A comparison between CSO and CLO as the major resin component showed that composites made from CLO exhibited better overall properties than those made with CSO. The Soxhlet extraction experiments, along with the ^{1}H-NMR spectra of the extracts, demonstrate that most of the monomers used were fully incorporated into the cured resin, with the exception of the conjugated oils.

The authors thank the Missouri Crop Improvement Association for the rice hulls, Professor Michael Kessler from the Department of Material Sciences and Engineering and Dr. Richard Hall from the Department of Natural Resource Ecology and Management at Iowa State University for the use of their facilities, Warren Straszheim from the Department of Material Sciences and Engineering for help with the SEM, and Dr. Douglas Stokke from the Department of Natural Resource Ecology and Management for important information concerning the rice hulls.

References

1. Ashraf, S. M.; Ahmad, S.; Riaz, U. Polym Int 2007, 56, 1173.
2. Mosiewicki, M.; Borrajo, J.; Aranguren, M. I. Polym Int 2007, 56, 779.
3. Sharma, V.; Banait, J. S.; Kundu, P. P. J Appl Polym Sci 2009, 114, 446.
4. Sharma, V.; Banait, J. S.; Kundu, P. P. J Appl Polym Sci 2009, 111, 1816.
5. Gultekin, M.; Beker, U.; Guner, F. S.; Erciyes, A. T.; Yagci, Y. Macromol Mater Eng 2000, 283, 15.
6. Sharma, H. O.; Alam, M.; Riaz, U.; Ahmad, S.; Ashraf, S. M. Int J Polym Mater 2007, 56, 437.
7. Wang, C.; Yang, L.; Ni, B.; Shi, G. J Appl Polym Sci 2009, 114, 125.
8. Thulasiraman, V.; Rakesh, S.; Sarojadevi, M. Polym Compos 2009, 30, 49.
9. Bhuyan, S.; Holden, L. S.; Sundararajan, S.; Andjelkovic, D.; Larock, R. C. Wear 2007, 263, 965.
10. Henna, P. H.; Andjelkovic, D. D.; Kundu, P. P.; Larock, R. C. J Appl Polym Sci 2007, 104, 979.
11. Lima, D. G.; Soares, V. C. D.; Ribeiro, E. B.; Carvalho, D. A.; Cardoso, E. C. V.; Rassi, F. C.; Mundim, K. C.; Rubim, J. C.; Suarez, P. A. Z. J Anal Appl Pyrolysis 2004, 71, 987.
12. Larock, R. C.; Dong, X.; Chung, S.; Reddy, C. K.; Ehlers, L. E. J Am Oil Chem Soc 2001, 78, 447.
13. Kundu, P. P.; Larock, R. C. Biomacromolecules 2005, 6, 797.
14. Xia, Y.; Henna, P. H.; Larock, R. C. Macromol Mater Eng 2009, 294, 590.
15. Andjelkovic, D. D.; Larock, R. C. Biomacromolecules 2006, 7, 927.
16. Andjelkovic, D. D.; Lu, Y.; Kessler, M. R.; Larock, R. C. Macromol Mater Eng 2009, 294, 472.
17. Valverde, M.; Andjelkovic, D.; Kundu, P. P.; Larock, R. C. J Appl Polym Sci 2008, 107, 423.
18. Pfister, D. P.; Larock, R. C. Bioresour Technol 2010, 101, 6200.
19. Quirino, R. L.; Larock, R. C. J Appl Polym Sci 2009, 112, 2033.
20. Bhuyan, S.; Sundararajan, S.; Pfister, D.; Larock, R. C. Tribol Int 2010, 43, 171.
21. Pfister, D. P.; Baker, J. R.; Henna, P. H.; Lu, Y.; Larock, R. C. J Appl Polym Sci 2008, 108, 3618.
22. Teng, H.; Wei, Y. Ind Eng Chem Res 1998, 37, 3806.
23. Srebrenkoska, V.; Gaceva, G. B.; Dimeski, D. Maced J Chem Chem Eng 2009, 28, 99.
24. Quirino, R. L.; Larock, R. C. J Appl Polym Sci, (DOI 10.1002/app.33630).
25. Barneto, A. G.; Carmona, J. A.; Alfonso, J. E. M.; Alcaide, L. J. Bioresour Technol 2009, 100, 3963.